

Spontaneous Shrinkage of Drops and Mass Conservation in Phase-Field Simulations

Pengtao Yue^{1,2}, Chunfeng Zhou¹ and James J. Feng^{1,2*}

¹Department of Chemical and Biological Engineering
University of British Columbia, Vancouver, BC V6T 1Z3, Canada

²Department of Mathematics
University of British Columbia, Vancouver, BC V6T 1Z2, Canada

Abstract - In this note we examine the implications of Cahn-Hilliard diffusion on mass conservation when using a phase-field model for simulating two-phase flows. Even though the phase-field variable ϕ is conserved globally, a drop shrinks spontaneously while ϕ shifts from its expected values in the bulk phases. Those changes are found to be proportional to the interfacial thickness, and we suggest guidelines for minimizing the loss of mass. Moreover, there exists a critical radius below which drops will eventually disappear. With a properly chosen mobility parameter, however, this process will be much slower than the physics of interest and thus has little ill effect on the simulation.

*Corresponding author. E-mail jfeng@CHML.UBC.CA

1 Introduction

In recent years, the phase-field model has gained popularity in simulating two-phase flows of immiscible fluids [1–6], and the method is the subject of several review articles [7–9]. In this framework, the fluid interface is treated as a thin but diffuse layer where the two components mix to some extent. The interfacial profile of a suitably defined phase-field variable ϕ is governed by a convection-diffusion equation, and the interfacial tension is recovered from the interfacial mixing energy. The advantages and limitations of the phase-field method, in relationship to other interface-capturing methods, have been discussed before [9,10]. In this note we focus on a question often asked of previous methods: how well does the method conserve mass? Since we consider incompressible fluids only, mass and volume conservation are used synonymously.

Phase-field methods come in two flavors: the non-conservative Allen-Cahn model and the conservative Cahn-Hilliard model. The former relies on an extra constraint to maintain mass conservation [11,12]. We are concerned here only with the latter, which assumes the diffusion to be driven not by $\nabla\phi$ but by the gradient of the chemical potential. This leads to the celebrated Cahn-Hilliard equation:

$$\frac{\partial\phi}{\partial t} + \mathbf{v} \cdot \nabla\phi = \gamma\Delta\mu, \quad (1)$$

where the chemical potential $\mu = \frac{\delta\mathcal{F}}{\delta\phi}$ is defined from the mixing energy \mathcal{F} in the whole domain, \mathbf{v} is the flow velocity and γ is a mobility parameter. With appropriate boundary conditions ($\mathbf{n} \cdot \mathbf{v}|_{\partial\Omega} = 0$ and $\mathbf{n} \cdot \nabla\mu|_{\partial\Omega} = 0$, where $\partial\Omega$ is the boundary of computation domain Ω and \mathbf{n} is the normal to $\partial\Omega$), the integration of Eq. (1) over Ω yields

$$\frac{d}{dt} \int_{\Omega} \phi \, d\Omega = 0, \quad (2)$$

which means that Cahn-Hilliard dynamics conserves mass over the entire domain. Since ϕ takes on constant values in the bulk of each component (± 1 , say), this further implies conservation of mass for each component provided that the interfacial layer is thin. Thus, the difficulty that requires special attention in level-set and volume-of-fluid methods appears to be nonexistent for the phase-field method.

In actual implementation, volume conservation is in fact an issue because the interface has a small but finite thickness. As the interface is the level set $\phi = 0$, the volume of a drop is liable to variations as the $\phi(\mathbf{r})$ field evolves. Theoretically, such variations vanish as the interfacial thickness approaches zero. In practice, the question is how to maintain mass conservation within an acceptable margin given a finite interfacial thickness. We have found hints in the literature on choosing parameters to balance the convective and diffusive tendencies in the Cahn-Hilliard dynamics [1], but no detailed discussion on the factors that affect mass conservation, much less an explicit criterion on ensuring it. This note aims to address this issue.

Two factors drive the evolution of ϕ : flow and diffusion. An external flow may take on any form and magnitude, and its effect on ϕ is difficult to analyze in generic terms. Yue

et al. [5] have touched on such flow effects in shear-induced drop deformation. Cahn-Hilliard diffusion is governed by an overall energy optimization, and is the fundamental mechanism for evolving ϕ . A well-known example of this mechanism at work is the assimilation of a smaller drop by a larger one nearby [3]. Therefore, we have chosen to analyze the simple situation of a single drop that shrinks spontaneously in a quiescent fluid. The insights gained from this exercise will apply to flow situations.

2 Spontaneous shrinking of a drop

For the mixing energy of the two-phase system, we adopt the Ginzburg-Landau functional:

$$\mathcal{F} = \int_{\Omega} \lambda \left[\frac{1}{2} |\nabla \phi|^2 + f(\phi) \right] d\Omega, \quad (3)$$

where λ is the mixing energy density and $f(\phi)$ is a double well potential $f(\phi) = \frac{(\phi^2-1)^2}{4\epsilon^2}$, ϵ being the capillary width indicative of the interfacial thickness. In the simplest case of a planar interface separating two unbounded components, energy minimization readily yields a one-dimensional (1D) equilibrium with $\phi = \pm 1$ in the two bulk phases and $\phi(x) = \tanh(\frac{x}{\sqrt{2}\epsilon})$ across the interface located at $x = 0$. If one takes $-0.9 < \phi < 0.9$ to be the extent of the interface, this ϕ profile gives an interfacial thickness of 4.164ϵ . The feasibility of a diffuse-interface approximation for two-phase flows with practically sharp interfaces rests on the fact that the bulk components are identified by $\phi = \pm 1$ and the interface is well defined at $\phi = 0$.

These fundamental precepts may come under doubt for more complex geometries. The requirement of $\phi = \pm 1$ in the bulk essentially depends on the interface having negligible volume compared to the bulk so that $f(\phi)$ alone matters in the energy minimization. This is the case for the planar interface discussed above, but not for a drop submerged in a matrix fluid in a finite domain, for example. This can be easily illustrated by considering the 2D schematics in Fig. 1, where we impose the hypertangent profile for 1D equilibrium along the radial direction with $\phi = \pm 1$ in the bulk phases. Thus, the free energy is concentrated on the interface, which is effectively the interfacial tension, with zero energy in the bulk. Because of the finite volume of the bulk, possibly the total energy can be reduced by shrinking the drop while simultaneously shifting the bulk ϕ slightly away from the initial values, as illustrated in Fig. 1(b). This amounts to reducing the interfacial energy at the expense of raising the bulk energy, which is perfectly permissible within the Cahn-Hilliard framework but would violate mass conservation for the drop in the physical context.

Such shifting of the interface is not because of the particular initial condition, in this case the hypertangent ϕ profile across the interface. In fact, Yue *et al.* [5, 9] have used the relaxed ϕ field, i.e., the 2D equilibrium state for a quiescent drop, as the initial condition in simulating shear-induced drop deformation. But as soon as the interfacial profile is perturbed, by flow in this case, the exchange between interfacial and bulk energies will potentially shift the location of the interface and cause volume loss of the drop. The phenomenon has also been noted by Jacqmin [1]. Thus, it is a fundamental mechanism

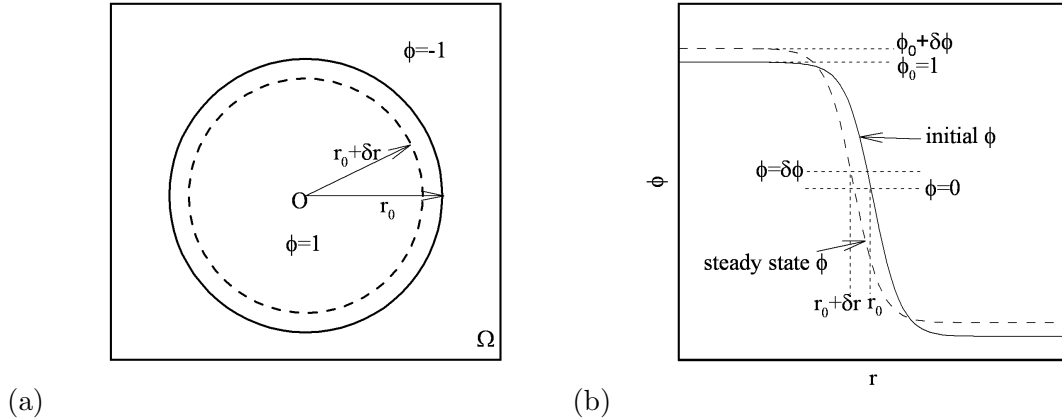


Figure 1: Schematic of the shrinkage of a circular drop in a quiescent matrix.

inherent to the Cahn-Hilliard dynamics. For ease of discussion and without loss of generality, we will consider only the shrinkage of a drop in a quiescent matrix with an initial condition that consists of the hypertangent profile along the radial direction and $\phi = \pm 1$ in the bulk.

2.1 Theoretical analysis

Multiplying Eq. (1) with μ and integrating over the whole computational domain Ω , we obtain the following energy law:

$$\frac{d\mathcal{F}}{dt} = -\gamma \int_{\Omega} (\nabla\mu)^2 d\Omega \leq 0, \quad (4)$$

where we have used the natural boundary condition $\mathbf{n} \cdot \nabla\phi|_{\partial\Omega} = 0$ and zero flux condition $\mathbf{n} \cdot \nabla\mu|_{\partial\Omega} = 0$. So the Cahn-Hilliard dynamics always tends to minimize \mathcal{F} , and the drop shrinks because the relaxed drop shape enjoys a lower energy. The shift of ϕ can be estimated based on an energy argument.

We consider a 2D circular drop as shown in Fig. 1. It is convenient to divide the total energy of Eq. (3) into an interfacial energy \mathcal{F}_1 (integration over the interfacial region) and a bulk energy \mathcal{F}_2 (integration over the two bulk regions). Then for the initial hypertangent ϕ profile, $\mathcal{F}_2 = 0$ and $\mathcal{F}_1 = \sigma S$, where $S = 2\pi r_0$ is the perimeter of the drop and σ is the interfacial tension. In the sharp interface limit $\sigma = \frac{2\sqrt{2}\lambda}{3\epsilon}$.

Under the constraint of Eq. (2), a variation in the drop radius δr must be accompanied by a shift $\delta\phi$ in the bulk ϕ values. We assume that the interface is very thin ($\epsilon \ll r_0$) and the shift $\delta\phi$ is uniform and equal in the two bulk components. To justify the latter, we note that ϕ is uniform in each bulk phase and the chemical potential $\mu = \lambda \frac{(\phi^2 - 1)\phi}{\epsilon^2}$. The spatial uniformity of μ in equilibrium then requires that the small shifts from $\phi = \pm 1$ be equal in

the two bulk phases. Thus, we obtain the relation between $\delta\phi$ and δr :

$$\delta\phi \approx -\frac{2S\delta r}{V} = -\frac{4\pi r_0\delta r}{V}, \quad (5)$$

where V is the volume of the whole computational domain Ω . In this equation and hereafter, we only keep the leading order terms. Now the interfacial energy will be changed due to the change in interfacial length:

$$\delta\mathcal{F}_1 \approx \sigma\delta S = 2\pi\sigma\delta r, \quad (6)$$

where we have neglected the variation in σ : $\delta\sigma \sim \int_{-\epsilon}^{\epsilon} \lambda\delta f dx \sim \sigma\delta\phi^2$. The bulk energy will be changed as well because ϕ shifts away from ± 1 :

$$\delta\mathcal{F}_2 \approx \int_{\Omega} \lambda\delta f d\Omega \approx \lambda\frac{\delta\phi^2}{\epsilon^2}V. \quad (7)$$

Combining Eqs. (5–7), we write the variation of the total mixing energy as:

$$\delta\mathcal{F} \approx 2\pi\sigma\delta r + \lambda\frac{(4\pi r_0)^2}{V\epsilon^2}\delta r^2. \quad (8)$$

Note that $\frac{\lambda}{\epsilon} \sim \sigma = O(1)$, and $\frac{\delta r}{\epsilon}$ will turn out to be $O(1)$ as well (see below). Thus, the second term $\delta\mathcal{F}_2 = O(\delta r)$ is of the same order as the first despite the quadratic form.

Since $\left.\frac{\partial(\delta\mathcal{F})}{\partial(\delta r)}\right|_{\delta r=0} = 2\pi\sigma > 0$, the total energy will be lowered by drop shrinkage ($\delta r < 0$). This justifies our conjecture in the previous section. It is also obvious from the fact that the increase in bulk energy is of order δr^2 whereas the reduction in interfacial energy is $O(\delta r)$. Furthermore, $\frac{\partial(\delta\mathcal{F})}{\partial(\delta r)} = 0$ gives the state of lowest energy and therefore the final shrinkage of the drop:

$$\delta r = -\frac{\sigma V}{16\pi\lambda} \left(\frac{\epsilon}{r_0}\right)^2 = -\frac{\sqrt{2}V}{24\pi} \frac{\epsilon}{r_0^2}, \quad (9)$$

or in dimensionless form:

$$\frac{\delta r}{r_0} = -\frac{\sqrt{2}}{24} \left(\frac{V}{V_d}\right) \left(\frac{\epsilon}{r_0}\right), \quad (10)$$

where $V_d = \pi r_0^2$ is the volume of drop. Substitute Eq. (9) into Eq. (5), we get the shift of ϕ :

$$\delta\phi = \frac{\sqrt{2}}{6} \frac{\epsilon}{r_0}. \quad (11)$$

For a spherical drop in three dimensions, similar results can be obtained:

$$\left(\frac{\delta r}{r_0}\right) = -\frac{\sqrt{2}}{18} \left(\frac{V}{V_d}\right) \left(\frac{\epsilon}{r_0}\right), \quad (12)$$

and

$$\delta\phi = \frac{\sqrt{2}}{3} \frac{\epsilon}{r_0}, \quad (13)$$

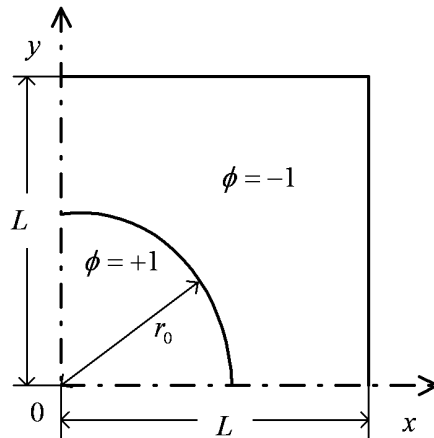


Figure 2: Computational domain for the finite element calculations. Symmetry conditions are imposed at the two axes. On the outer boundaries $\mathbf{n} \cdot \nabla \phi = 0$ and $\mathbf{n} \cdot \nabla \mu = 0$.

where $V_d = \frac{4}{3}\pi r_0^3$ is the volume of the spherical drop.

Note that we have neglected terms of higher order than $\delta r/r_0$ and $\delta \phi$ in the above. Thus, the validity of Eqs. (10–13) requires $\frac{\delta r}{r_0} \ll 1$, which is more restrictive than $\frac{\epsilon}{r_0} \ll 1$ as $\frac{V}{V_d} > 1$. In the literature, $Cn = \frac{\epsilon}{r_0}$ is defined as the Cahn number. In addition, we have assumed $\phi = 1$ inside the drop and $\phi = -1$ outside. If this is reversed, $\delta \phi$ in Eqs. (11) and (13) takes on a minus sign while δr in Eqs. (10) and (12) does not change.

2.2 Numerical verification

To verify the above analysis, we have performed numerical simulations of the spontaneous shrinking of 2D and 3D drops. In 2D, we use a Fourier-Chebyshev Galerkin spectral method [5] in a rectangular box of $2\pi \times 2$, with periodicity in the horizontal direction. Drops with initial radius $r_0 = 0.25, 0.4, 0.5, 0.52, 0.6, 0.7, 0.8$ and 0.9 and capillary width $\epsilon = 0.01$ and 0.02 are simulated. In addition, we use a finite-element code with adaptive meshing [6] to compute shrinking of 2D and axisymmetric 3D drops. The computational domain is shown in Fig. 2 with $L = 2$. Thus $V = 16$ for the 2D and $V = 16\pi$ for the 3D domain. The initial drop radius is fixed at $r_0 = 1$ and a range of capillary widths is tested: $\epsilon = 0.005, 0.01, 0.02, 0.05, 0.1$ and 0.2 . For all the calculations, we initially set $\phi = +1$ inside the drop and $\phi = -1$ outside. Mesh size at the interface is roughly $\frac{\epsilon}{2}$ to guarantee numerical accuracy.

Figure 3 compares the numerical and theoretical results of $\delta \phi$ and $\delta r/r_0$. In the numerical results, $\delta \phi$ is spatially uniform for smaller values of the Cahn number Cn . At $Cn = 0.05$, for instance, the variation is below 3.1% over the computational domain in 2D. With increasing Cn , the spatial variation of $\delta \phi$ becomes more substantial. Thus, we take $\delta \phi$ to be $\frac{1}{2}[(\phi_{max} - 1) + (\phi_{min} + 1)]$. The comparison shows excellent agreement between numerical simulations and theory for relatively small values of Cn , while toward the upper end of the Cn range, deviations start to appear as the analytical result loses accuracy.

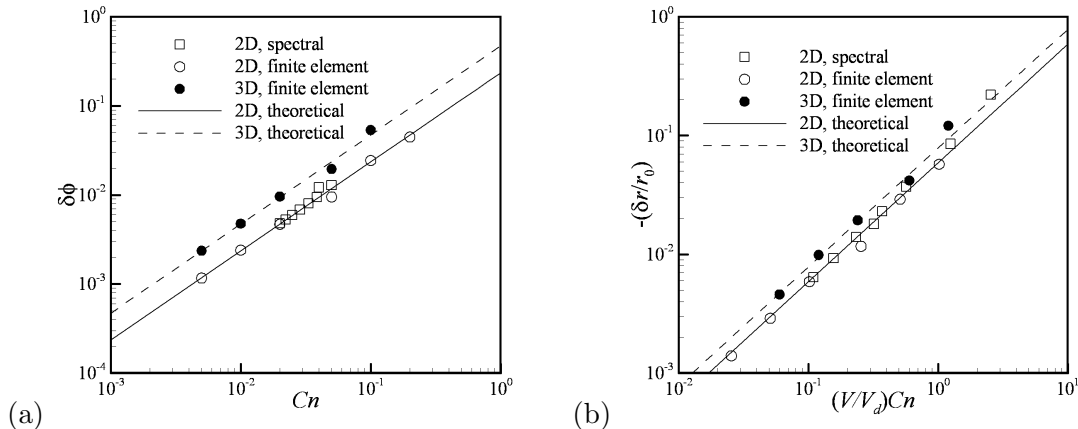


Figure 3: Comparison between theoretical and numerical results on (a) shift of the phase field variable ϕ and (b) shrinkage of the drop radius.

2.3 Guidelines for conserving mass

Equations (10–13) lead to the following guidelines for conserving mass for each component in phase-field simulations. First, use a small Cahn number $Cn \ll 1$. This amounts to the requirement that ϵ be much smaller than drop size. Based on 1D solidification calculations, Fabbri and Voller [13] suggested that ϵ should be smaller than 0.0025 of the domain size. Our experience indicates that $Cn \lesssim 0.01$ is generally sufficient. Second, avoid using very large computational domains relative to the size of the dispersed phase. If the volume ratio V/V_d is large, a drop may shrink considerably even for a small Cn . In fact, drops with an initial size below a critical size will disappear altogether (see Section 3). Again, these guidelines apply to flow situations as well despite the fact that they have been developed here in the simpler case of no external flows.

Two interesting comments may be made on the condition $Cn \ll 1$. First, this is the condition for approaching the sharp-interface limit. Taking a diffuse interface as an approximation of the sharp interface, it is easy to show that the error in the interfacial tension is $O(Cn^2)$, and the error in mixture properties such as density and viscosity is $O(Cn)$. Thus, the requirement of mass conservation partially overlaps with that for approximating the sharp-interface situation. Thinner interfaces are computationally more costly to resolve, of course. Our recent work has shown adaptive meshing as an attractive strategy for reaching down to smaller values of Cn [6]. Second, the Cahn number should be understood more generally as the ratio between ϵ and the smallest length scale of interest. In singular events such as interfacial rupture and coalescence, the local radius of curvature approaches zero, or more appropriately ϵ , since no interfacial feature below ϵ is meaningful in the diffuse-interface context. Thus, $Cn \rightarrow 1$ no matter how small ϵ is. One may view this as the failure of the phase-field method since its convergence to the sharp-interface limit breaks down. However, such events are dominated by short-range forces and the classical sharp interface model cannot represent the real physics either. In fact, the phase-field model contains a

phenomenological “short-range force” that resembles the van der Waals force [14]. In this sense, the phase-field model is superior in treating such singular events.

3 Critical drop radius

Equations (10) and (12) suggest that a drop may disappear completely when $\frac{V}{V_d} \frac{\epsilon}{r_0}$ is large enough. But this is inconclusive since these equations hold only for $\delta r \ll r_0$. In the following, we present an alternative analysis that establishes a critical drop radius r_c such that all the drops with $r_0 < r_c$ will disappear eventually in a process analogous to Ostwald ripening. The only assumption is $\epsilon \ll r_0$ or $Cn \ll 1$.

Consider a 2D drop of initial radius r_0 with $\phi = 1$ inside the drop and $\phi = -1$ outside. When the drop radius shrinks to r , we again assume an equal and uniform shift $\delta\phi$ inside and outside. The conservation of ϕ over the entire domain gives:

$$\delta\phi = \frac{2\pi(r_0^2 - r^2)}{V}. \quad (14)$$

Although $r_0^2 - r^2$ is now finite, it can be confirmed a posteriori using Eq. (17) that $\delta\phi \sim \frac{r_0^2}{V} \sim \frac{(V\epsilon)^{2/3}}{V} = \frac{\epsilon^{2/3}}{V^{1/3}} \ll 1$. Neglecting cubic and quartic terms in $\delta\phi$, we write the total free energy at drop radius r as:

$$\begin{aligned} \mathcal{F} &\approx 2\pi r\sigma + \lambda \frac{[(1 + \delta\phi)^2 - 1]^2}{4\epsilon^2} (\pi r^2) + \lambda \frac{[(-1 + \delta\phi)^2 - 1]^2}{4\epsilon^2} (V - \pi r^2) \\ &\approx \frac{4\sqrt{2}\pi}{3} \frac{\lambda}{\epsilon} r + 4\pi^2 \frac{\lambda}{\epsilon} \frac{1}{V\epsilon} (r_0^4 - 2r_0^2 r^2 + r^4), \end{aligned} \quad (15)$$

where we have tacitly assumed $r \gg \epsilon$ and approximated the interfacial tension by the asymptotic formula. Although a vanishing drop eventually has its radius reduced to $r \sim \epsilon$, we will find below that the r of interest in our analysis is $O(r_0)$.

Now the derivative of \mathcal{F} with respect to r is:

$$\frac{\partial \mathcal{F}}{\partial r} = \frac{4\sqrt{2}\pi}{3} \frac{\lambda}{\epsilon} + 4\pi^2 \frac{\lambda}{\epsilon} \frac{1}{V\epsilon} (4r^3 - 4r_0^2 r). \quad (16)$$

Since $\frac{\partial \mathcal{F}}{\partial r}|_{r=0} = \frac{\partial \mathcal{F}}{\partial r}|_{r=r_0} > 0$, the $\mathcal{F}(r)$ curve must have an inflexion point at $r_i \in [0, r_0]$ as shown in Fig. 4; r_i is readily calculated from $\frac{\partial^2 \mathcal{F}}{\partial r^2} = 0$: $r_i = \frac{\sqrt{3}}{3} r_0$. If $\frac{\partial \mathcal{F}}{\partial r}|_{r=r_i} < 0$, the energy $\mathcal{F}(r)$ will exhibit a potential well at some $r_w > r_i$. Then the shrinking drop will be trapped at r_w and will not vanish even if $\mathcal{F}(r = 0) < \mathcal{F}(r = r_0)$. Therefore a vanishing drop requires $\frac{\partial \mathcal{F}}{\partial r}|_{r=r_i} \geq 0$, which is satisfied by

$$r_0 \leq r_c = \left(\frac{\sqrt{6}}{8\pi} V\epsilon \right)^{1/3}. \quad (17)$$

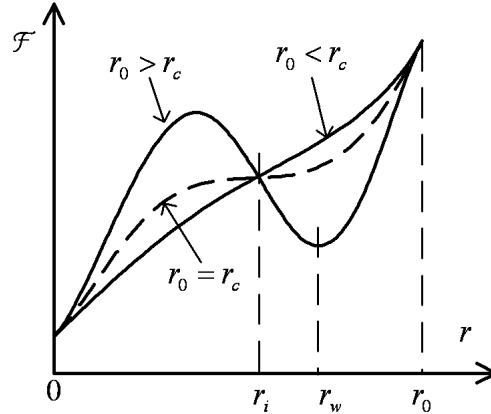


Figure 4: Schematic of the mixing energy \mathcal{F} as a function of drop radius r . The dashed curve with $r_0 = r_c$ has zero slope at $r = r_i$.

Drops with initial radius r_0 below the critical radius r_c will eventually disappear. Similar results may be derived for 3D drops: $r_i = \frac{r_0}{2^{2/3}}$ and

$$r_c = \left(\frac{2^{1/6}}{3\pi} V \epsilon \right)^{1/4}. \quad (18)$$

These formulae have been verified by finite-element computations, and the results are plotted in Fig. 5.

Equations (17) and (18) indicate that r_c is largely determined by the domain size, and only depends on ϵ weakly. Once the domain size is chosen, there is little room for raising r_c by reducing the capillary width ϵ . Fortunately, r_c does not necessarily set the minimum feature size that may be simulated. If the time scale of interest t_f , e.g. related to flow or interfacial deformation, is much shorter than the shrinkage time t_{sh} , then the process can be computed accurately with minimal loss of mass even for $r_0 < r_c$. This depends on the Cahn number Cn as well as the mobility parameter γ .

To estimate the shrinkage time t_{sh} , we write the Cahn-Hilliard diffusion flux as $F = \gamma \nabla \mu$. The chemical potential μ may be estimated as the phase-field analogue of interfacial tension times curvature [1]: $\mu \sim \frac{\sigma}{r_0}$. The length scale l over which μ varies is much larger than ϵ ; it may be estimated by scaling arguments [15], but will be determined below from numerical data. Now we have $F \sim \frac{\gamma \sigma}{r_0 l}$. When the radius shrinks by Δr in time t_{sh} , the “mass” of ϕ that passes through unit area of the interface is $\Delta r = F t_{sh}$, which gives

$$t_{sh} \sim \frac{r_0 \Delta r l}{\gamma \sigma}. \quad (19)$$

Comparing this scaling with numerical data shows that for the few ϵ values tested, $\frac{l}{\epsilon}$ is on the order of 100:

$$t_{sh} \approx 100 \frac{r_0 \Delta r \epsilon}{\gamma \sigma}. \quad (20)$$

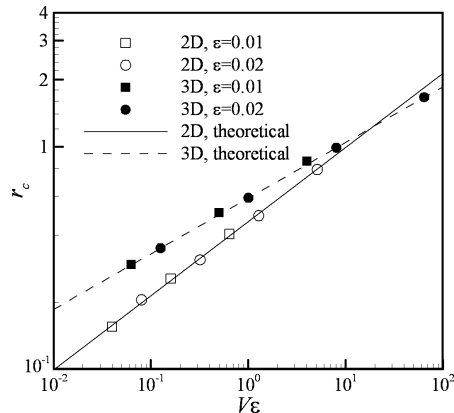


Figure 5: Comparison between theoretical and numerical results on the critical drop radius r_c . The range of V is achieved by using $L = 1, 2, 4$ and 8 in the computational domains (see Fig. 2). Numerically, discrete r_0 values are tested to bracket r_c within 3%.

Comparing the diffusive and convective fluxes, Jacqmin [1] suggested a scaling for the mobility $\gamma \sim \epsilon^n$ with n between 1 and 2. In our simulations of flow-induced drop deformation, we have found $\gamma \sim Gr_0\epsilon^2/\sigma$ to be a good choice, G being the characteristic strain rate. Substituting this γ into Eq. (20) gives

$$t_{sh} \approx 100 \frac{\Delta r}{r_0} \frac{r_0}{\epsilon} \frac{1}{G} = 100 \frac{\Delta r}{r_0} Cn^{-1} G^{-1}. \quad (21)$$

Therefore, the time needed for the drop to shrink by a significant fraction is at least two orders of magnitude longer than the flow time $t_f = G^{-1}$. The smaller the Cahn number Cn , the greater the disparity between t_{sh} and t_f . In other words, by using a small Cn and a judicious choice of the γ parameter, drop shrinkage can be kept under control even for small drops with $r_0 < r_c$.

This conclusion has been borne out by numerical simulations of drop deformation in elongational flow (see Ref. [6] for details). The axisymmetric computational domain has $L = 10$ (see Fig. 2), and the other parameters are $r_0 = 1$, $\epsilon = 0.01$, $G = 1$, and $\sigma = 10$. We have chosen $\gamma = 2.0 \times 10^{-5} \sim Gr_0\epsilon^2/\sigma$. Equation (18) gives $r_c = 1.65 > r_0$ so the drop is subject to disappearance. As an example, a drop of equal viscosity to the external fluid achieves a steady-state spheroidal shape in a flow time of $t_f \approx 5$. The shrinkage time from Eq. (20) is $t_{sh} \approx 5000 \gg t_f$. At $t = 5$, the drop volume has decreased by 1.4%, equivalent to a decrease in the effective radius of 0.5%. Therefore, mass is conserved to a great degree of accuracy even though we are calculating a drop smaller than the critical one, and the numerical result agrees well with the sharp-interface result.

4 Summary

In this note, we have demonstrated that the shift of the phase-field variable ϕ and shrinkage of drops are phenomena inherent to the Cahn-Hilliard dynamics. The shift $\delta\phi$ and drop shrinkage δr are calculated and turn out to be proportional to the Cahn number $Cn = \frac{\epsilon}{r_0}$. Based on these, guidelines are suggested for maintaining mass conservation in phase-field simulations of two-phase flows. In particular, the mass loss becomes negligible if a small enough capillary width ϵ is used. Although the results are derived for a specific set of initial conditions in the absence of external flow, the guidelines are general.

Furthermore, there exists a critical drop radius r_c for a given computational domain and capillary width so that drops smaller than r_c will eventually vanish. This r_c could be rather large for large computational domains. Fortunately, with the proper choice of the mobility parameter γ and a small enough ϵ , drop shrinkage can be very slow and thus causes little loss of mass during the time of interest based on global dynamics.

Acknowledgment: Acknowledgment is made to the Donors of The Petroleum Research Fund, administered by the American Chemical Society, for partial support of this research. J.J.F. was also supported by the NSERC, the Canada Research Chair program and the Canada Foundation for Innovation. C.Z. acknowledges partial support by a University Graduate Fellowship from UBC. We thank Chun Liu and Jie Shen for helpful discussions.

References

- [1] D. Jacqmin, Calculation of two-phase Navier-Stokes flows using phase-field modelling, *J. Comput. Phys.* 155 (1999) 96–127.
- [2] B. J. Keestra, P. C. J. van Puyvelde, P. D. Anderson, H. E. H. Meijer, Diffuse interface modeling of the morphology and rheology of immiscible polymer blends, *Phys. Fluids* 15 (2003) 2567–2575.
- [3] C. Liu, J. Shen, A phase field model for the mixture of two incompressible fluids and its approximation by a Fourier-spectral method, *Physica D* 179 (2003) 211–228.
- [4] V. E. Badalassi, H. D. Ceniceros, S. Banerjee, Computation of multiphase systems with phase field model, *J. Comput. Phys.* 190 (2003) 371–397.
- [5] P. Yue, J. J. Feng, C. Liu, J. Shen, A diffuse-interface method for simulating two-phase flows of complex fluids, *J. Fluid Mech.* 515 (2004) 293–317.
- [6] P. Yue, C. Zhou, J. J. Feng, C. F. Ollivier-Gooch, H. H. Hu, Phase-field simulations of interfacial dynamics in viscoelastic fluids using finite elements with adaptive meshing, *J. Comput. Phys.* 219 (2006) 47–67.
- [7] J. Lowengrub, L. Truskinovsky, Quasi-incompressible Cahn-Hilliard fluids and topological transitions, *Proc. Roy. Soc. Lond. A* 454 (1998) 2617–2654.

- [8] D. M. Anderson, G. B. McFadden, A. A. Wheeler, Diffuse-interface methods in fluid mechanics, *Ann. Rev. Fluid Mech.* 30 (1998) 139–165.
- [9] J. J. Feng, C. Liu, J. Shen, P. Yue, An energetic variational formulation with phase field methods for interfacial dynamics of complex fluids: advantages and challenges, In M.-C. T. Calderer, E. Terentjev, editors, *Modeling of Soft Matter*, pages pp. 1–26. Springer, New York, 2005.
- [10] J. A. Sethian, P. Smereka, Level set methods for fluid interfaces, *Ann. Rev. Fluid Mech.* 35 (2003) 341–372.
- [11] T. Biben, C. Misbah, A. Leyrat, C. Verdier, An advected-field approach to the dynamics of fluid interfaces, *Europhys. Lett.* 63 (2003) 623–629.
- [12] X. Yang, J. J. Feng, C. Liu, J. Shen, Numerical simulations of jet pinching-off and drop formation using an energetic variational phase-field method, *J. Comput. Phys.* 218 (2006) 417–428.
- [13] M. Fabbri, V. R. Voller, The phase-field method in the sharp-interface limit: A comparison between model potentials, *J. Comput. Phys.* 130 (1997) 256–265.
- [14] P. Yue, J. J. Feng, C. Liu, J. Shen, Diffuse-interface simulations of drop coalescence and retraction in viscoelastic fluids, *J. Non-Newtonian Fluid Mech.* 129 (2005) 163–176.
- [15] A. J. Briant, J. M. Yeomans, Lattice Boltzmann simulations of contact line motion. II. Binary fluids, *Phys. Rev. E* 69 (2004) 031603.